crystals

MDPI

Article

Photoalignment and Photofixation of Chromonic Mesophase in Ionic Linear Polysiloxanes Using a Dual Irradiation System

Mitsuo Hara [1,*], Ayaka Masuda [1], Shusaku Nagano [2] and Takahiro Seki [1,*]

[1] Department of Molecular and Macromolecular Chemistry, Graduate School of Engineering, Nagoya University, Furo-cho, Chikusa-ku, Nagoya 464-8603, Aichi, Japan
[2] Department of Chemistry, College of Science, Rikkyo University, 3-34-1 Nishi-Ikebukuro, Toshima, Tokyo 171-8501, Japan
* Correspondence: mhara@chembio.nagoya-u.ac.jp (M.H.); tseki@chembio.nagoya-u.ac.jp (T.S.)

Abstract: Photoalignment technology enables macroscopic alignment of liquid crystalline molecules and their aggregates in a non-contact process by irradiating photo-responsive liquid crystalline compounds with linearly polarized light. Because photoalignment techniques prevent dust generation and uneven stretching, and accomplish fine and complex patterning, they are involved in the practical process of fabricating display panels, and continue to be applied in the research and creation of various anisotropic materials. Brilliant yellow (BY), a chromonic liquid crystal, has attracted considerable attention as the photoalignment sublayer in recent years, because of its ability to induce a high dichroic nature among many photo-responsive liquid crystalline materials. However, its dichroism is not maintained after prolonged exposure to a humid environment because of its intrinsic strong hygroscopicity of ionic BY molecules. In this study, to overcome this drawback, the photoalignment and successive photo-fixation of the BY columnar phase is proposed using UV-curable ionic polysiloxane as a matrix. Visible light was used for the photoalignment of the BY columnar phase, and UV light for photo-fixation. Consequently, the columnar chromonic phase is found to retain its orientation even after 4 h of exposure to a highly humid environment.

Keywords: chromonic liquid crystal; polysiloxane; photoalignment; UV curing

check for updates

Citation: Hara, M.; Masuda, A.; Nagano, S.; Seki, T. Photoalignment and Photofixation of Chromonic Mesophase in Ionic Linear Polysiloxanes Using a Dual Irradiation System. *Crystals* **2023**, *13*, 326. https://doi.org/10.3390/cryst13020326

Academic Editor: Borislav Angelov

Received: 4 February 2023
Revised: 10 February 2023
Accepted: 12 February 2023
Published: 15 February 2023

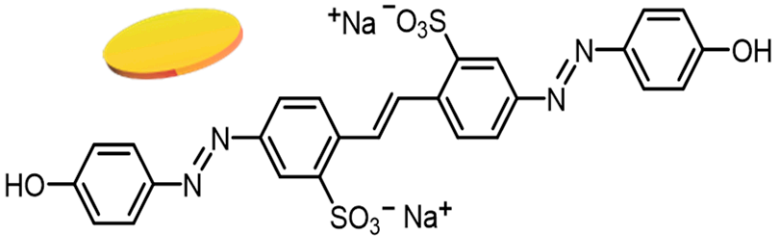
Copyright: © 2023 by the authors. Licensee MDPI, Basel, Switzerland. This article is an open access article distributed under the terms and conditions of the Creative Commons Attribution (CC BY) license (https://creativecommons.org/licenses/by/4.0/).

1. Introduction

Liquid crystals (LCs) self-assemble in response to temperature, electric fields, concentration, light irradiation, and other environmental conditions to form nano-periodic structures. Such soft materials are suitable for templates of nanostructures [1]. The dynamic cooperativity of LCs also facilitates control of the arrangement of molecules and their aggregates over a macroscopic scale, and enables their use in a variety of applications such as biosensors, optical devices, separators, and actuators [2–5]. Among them, lyotropic LCs mostly self-assemble in aqueous solvents, and they can be applied to various environmentally friendly processes. Some lyotropic LCs are classified as chromonic LCs [6–11]. Chromonic LCs are soft materials containing dye groups such as mesogens, which self-assemble to form columnar nanostructures via $\pi\pi$ interaction in solvents. The self-assembly structures that involve absorption anisotropy of chromonic LCs can be applied to optically functional films when the structures are align overlarge areas [12–15]. In particular, the optical manipulation of chromonic LC phases using photoalignment techniques [16–18] has the advantage of ready achievement of fine patterning, which is difficult to be accomplish by conventional mechanical rubbing or film stretching techniques [19–22].

Among chromonic LCs, brilliant yellow (BY) (as shown in Scheme 1) has attracted significant attention in recent years, and research using BY films as LC alignment sublayers has been extensively undertaken [23–38]. This is because the columnar LC phase of BY is well photoaligned using linearly polarized UV or visible light, creating highly dichroic optical films [39–42]. Such photoaligned BY films function well as alignment sublayers

for low-molecular-mass nematic LCs. However, BY exhibits a hygroscopic nature, which means that it cannot maintain dichroism for a long time in a highly humid environment. If the photoaligned BY columnar phase can be stabilized, it is anticipated that the high dichroic properties of BY could be used in more applications in wider variety situations; however, such a methodology has not yet been proposed.



Brilliant Yellow (BY)

Scheme 1. Chemical structure of chromonic liquid crystal used in this study.

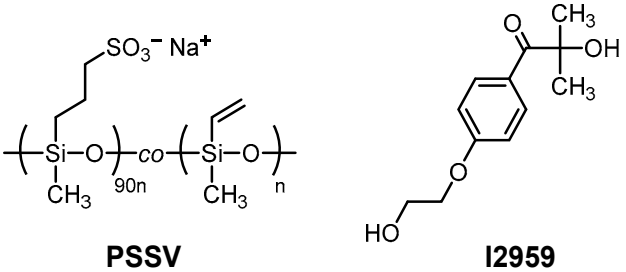
Matrix fixation by sol-gel reaction is often used in the stabilization of lyotropic LC phases [43,44]. However, chromonic LCs generally have low solubility in metallic-alkoxide sol (such as silica sol), and the addition of a compatibilizer is necessary to improve compatibility [14,45]. In addition, the chromonic LCs are solidified by the silica matrix through film formation, which makes photoalignment of BY after film formation difficult to achieve using conventional stabilization methods for lyotropic LCs.

Some recently developed ionic linear polysiloxanes are compatible with the hydrophilic region of lyotropic LC phases [46]. By introducing functional groups that can be cross-linked by ultraviolet light into polysiloxane, it is also possible to fix the LC phase in the matrix at targeted times and locations after film formation [47]. Conversion of the ionic groups of polysiloxanes is relatively easy, and a variety of ionic polysiloxanes can be prepared [48]. The ease of design of the ionic group of polysiloxanes means that development of an ionic polysiloxanes with high compatibility with chromonic LCs can be easy. In this study, the design for an ionic linear polysiloxane that is compatible with BY and has photo-crosslinking groups is proposed. By preparing a mixed thin film of the polysiloxane and BY, the photo-orientation of the BY columnar phase by visible light is demonstrated in the polysiloxane matrix. Subsequent fixation by UV light irradiation is also achieved. By photo-fixing the BY columnar phase, the dichroism ratio may be maintained even after extended exposure to a humid environment.

2. Materials and Methods

2.1. Materials

Scheme 2 shows the chemical structures used in this paper. BY chromonic dye and Irgacure® 2959 (I2959) photoinitiator were purchased from Sigma-Aldrich and Tokyo Chemical Industry (TCI), respectively. An anionic linear polysiloxane containing vinyl groups (PSSV) was synthesized via polycondensation of silane coupling agents. *N*, *N*-Dimethylformamide (DMF) was purchased from Kanto Chemical. The I2959 and DMF used were of commercial purity. Water was obtained through a Direct-Q® 3UV purification system (Millipore Corp., Burlington, MA, USA, ρ (resistivity) > 18 MΩ·cm at 25 °C).



PSSV **I2959**

Scheme 2. Chemical structures of hygroscopic siloxane copolymer and photoinitiator used in this study.

2.2. Synthesis of PSSV

PSSV was synthesized according to the scheme shown in Figure 3a [49]. The detailed procedure is follows.

1.8 g (1.0×10^{-2} mol) of 3-mercaptopropyl(dimethoxy)methylsilane (TCI) and 3.5×10^{-2} g (2.6×10^{-4} mol) of dimethoxymethylvinylsilane (TCI) were added to 54 g of 2 mol L^{-1} of sodium hydroxide (TCI). The mixture solution was stirred at 25 °C for 2 h before the addition of polysiloxane containing mercapto groups and vinyl groups. To oxidize the mercapto groups, 6 g of 30% hydrogen peroxide water (Kanto Chemical) was added to the mixture solution, and the resulting solution was stirred at 25 °C for 12 h. The solvent was dried using a smart evaporator C1 (BioChromato) and a white powder was obtained. The powder was dissolved in 300 mL of water, and ion exchange occurred using an ion-exchange resin Amberlite® IR120, in hydrogen form (Fluka). After the solution was treated using an ion-exchange resin IR120B Na (Organo) and dried using an evaporator, 2.1 g of white powder was obtained.

^{1}H NMR spectra of the product were recorded using a 400 MHz FT-NMR spectrometer JNM-A400 (JEOL). The spectrum is shown in Figure 3b. The molar ratio of each monomer unit in the copolymer was 90:1, which was calculated from the peak-integration ratio of peak d and f in the ^{1}H NMR spectrum.

2.3. Preparation of Pure BY Spin-Coated Films

BY was added to DMF (BY concentration: 1.5% by weight). The solution was heated in an oil bath at 150 °C for 4 h and allowed to cool before the undissolved portion was removed by filtration. Pure BY films were prepared by spin-coating the filtered solution onto the UV-O_3 treated quartz. The spin-coated films were prepared at 1500 rpm for 30 s. The relative humidity at the time of spin-coating was 14% (RH = 14%), as measured using an RTR-503 temperature and humidity recorder (T&D Corp.). The resulting films were then annealed at 120 °C for 10 min.

2.4. Preparation of BY-PSSV Spin-Coated Films

BY, PSSV, and I2959 were added to mixture of DMF and water. The weight ratio of the components was BY:PSSV:I2959:DMF:water = 1.2×10^1:3.0:6.0×10^{-2}:7.4×10^2:2.2×10^1. The solution was filtered to separate the undissolved portion. The BY-PSSV films were prepared using the filtered solution in the same way as the pure BY film. The resulting films were annealed at 120 °C for 10 min.

2.5. Film Thickness Measurement

Surface roughness was characterized by a white light interferometric BW-S507-N microscope (Nikon Corp., Tokyo, Japan). Bridgelements® was used for the software modules. To measure film thickness, the substrate was exposed by scratching the film with a micro spatula. Subsequently, the height difference between the top and bottom layer of the film was measured by a BW-S507-N microscope. The top-to-bottom height was taken as the film thickness.

2.6. Water Absorption Measurements

The hygroscopicity of pure BY and PSSV was evaluated by the quartz crystal microbalance (QCM) method. The QCM measurements were performed based on the methodology of previous research [50]. As PSSV exhibits high hygroscopicity, the QCM measurements could not guarantee accuracy when RH > 50%. Therefore, the water absorption of PSSV in the high humidity range was evaluated by the following method. Approximately 30 mg of PSSV was exposed to various humidity-controlled environments for several days. Once it reached an equilibrium moisture absorption state, its weight was measured. The relative humidity was controlled using a saturated aqueous solution of inorganic salts such as magnesium nitrate (RH ~50%), sodium chloride (RH ~65%), potassium chloride (RH ~80%), and potassium nitrate (RH ~88%). Experimental values of relative humidity realized in the saturated aqueous solutions of each inorganic salts are given in parentheses. All salts were purchased from Kishida Chemical and used as purchased.

2.7. Photoalignment of the BY Columnar Phase

The spin-coated films were placed on a homemade quartz chamber attached to the RTR-503 humidity sensor. The humidity in the chamber was controlled at approximately 15% using a me-40DP series precise dew-point generator (Micro Equipment). The spin-coated films in the chamber were exposed to linearly polarized visible (LPVis) light (436 nm) passed through a band pass filter and a polarizer using a mercury lamp REX-250 (Asahi Spectra) at room temperature. The light intensity at the sample position was 10 mW cm^{-2}.

Polarized UV-vis absorption spectra were taken on an Agilent 8453 spectrophotometer (Agilent Technologies). The orientation order parameter (S) of BY molecules is defined as $(A_{\perp} - A_{\parallel})/(A_{\mathrm{large}} + 2A_{\mathrm{small}})$, where $A_{\perp}$ and $A_{\parallel}$ are absorbances taken with perpendicular and parallel polarized probing beams, respectively. A_{large} and A_{small} represent the larger and smaller absorbances of the two measurements, respectively.

2.8. Evaluation of the Photoaligned BY Columnar Phase by X-ray Scattering Measurements

Grazing-incidence small-angle X-ray scattering (GI-SAXS) measurements were taken by an FR-E X-ray diffractometer equipped with a two-dimensional detector R-axis IV (Rigaku) involving an imaging plate (Fujifilm). An X-ray beam (Cu Kα = 0.154 nm, 0.3 mm collimated) was used, and the camera length was set at 300 mm. The spin-coated films were placed onto a pulse motor stage composed of oblique pulse (ATS-C310-EM, Chuo Precision Industrial) and Z-pulse (ALV-3005-HM, Chuo Precision Industrial) motors. The incident angle of the X-ray beam was adjusted between 0.18 and 0.22° to the substrate surface using the pulse motors.

2.9. UV-Curing of BY Columnar Phase

For UV-curing of the BY columnar phase, non-polarized UV light (365 nm, 5 mW cm^{-2}) passed through band pass filter from a REX-250 was irradiated to the spin-coated films for 5 min.

3. Results and Discussion

3.1. Photoalignment and Humidity Resistance of Pure BY Film

White interference microscopy images of BY films are shown in Figure 1a. The groove in the center of the image was formed when the film was scraped with a micro spatula. A smooth surface morphology with a film thickness of approximately 23 nm was obtained. Figure 1b shows the polarized UV-vis absorption spectrum of the BY film irradiated with LPVis light. The dichroism was induced upon LPVis irradiation. The order parameter (S) for the irradiation dose reached approximately 0.5 at 3 J cm^{-2}, and subsequent irradiation provided S = 0.7 after further dose (Figure 1c), indicating that BY is highly photoaligned by LPVis irradiation.

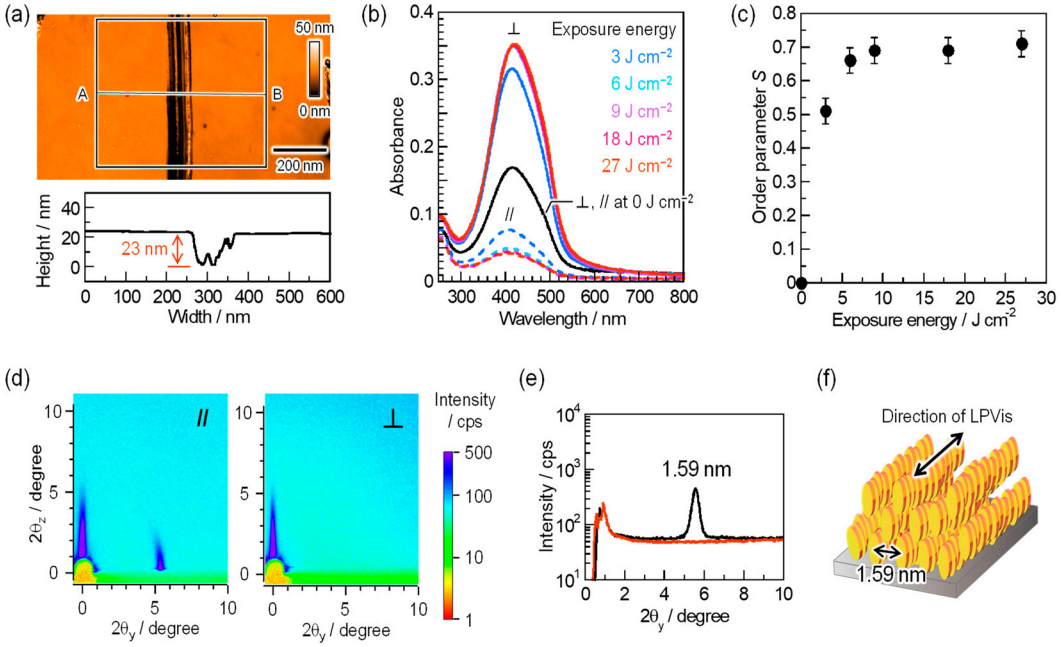


Figure 1. (**a**) Surface topographical morphology of pure BY film. The cross-section of the average height profile along the A-B line in the box is shown below. (**b**) Polarized UV-vis absorption spectra change of pure BY films associated with exposure to LPVis light. (**c**) Order parameter change associated with dose of visible light. (**d**) GI-SAXS images of pure BY films irradiated with LPVis light of 27 J cm^{-2} dose. (**e**) In-plane intensity profiles of d. (**f**) Photoaligned BY columnar phase.

Scattering images and in-plane intensity profiles obtained by GI-SAXS measurements of a BY film irradiated with 27 J cm^{-2} of LPVis light are shown in Figure 1d,e, respectively. When the X-rays were incident parallel to the direction of LPVis light, scattering with an in-plane spacing of 1.59 nm was observed in the in-plane direction, suggesting that the average distance between the columnar aggregates of BY was observed as the scattering peak [39]. Thus, the BY aggregates are uniformly oriented with the column axis parallel to the LPVis light, as shown in Figure 1f.

Figure 2 shows UV-visible spectral changes and *S* when the photoaligned the BY columnar phase was exposed to a high RH at 90%. A red shift occurred after 1 h of the humidification, and the *S* value decreased with further humidification. This can be ascribed to the fact that BY exhibits a hygroscopic nature, as shown in Figure 2c. The adsorbed water can cause an orientational relaxation of the hydrated the aggregates, leading to the deterioration of photoalignment.

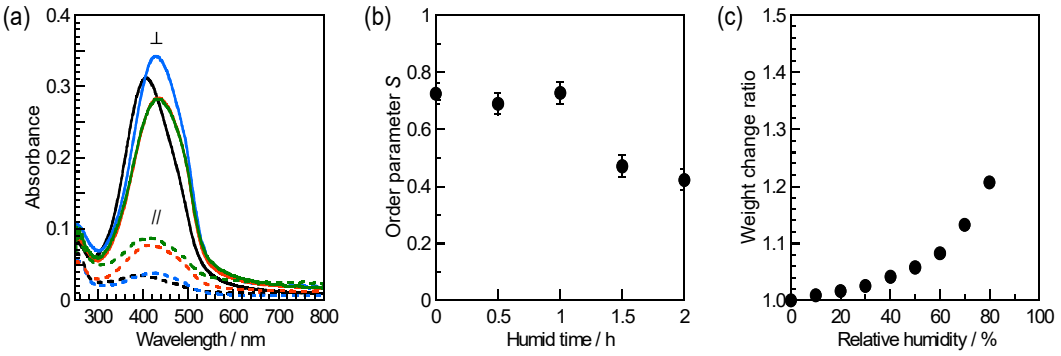


Figure 2. (**a**) Polarized UV-vis absorption spectra change with humidification at RH = 90% for photoaligned pure BY film. Black, blue, brown, and green lines indicate spectra after humidification of 0, 1, 1.5, and 2 h, respectively. (**b**) Order parameter change with humidification for photoaligned pure BY film. (**c**) Humidity-responsive weight change ratios of BY film prepared on a QCM electrode.

3.2. Hygroscopicity of Ionic Linear Polysiloxane Containing Sodium Sulfonate Groups

The ionic linear polysiloxane PSSV was used for the fixation of the BY columnar phase. Spin-coated films of PSSV were prepared on a QCM electrode substrate, and the weight change of the films was monitored upon humidification (Figure 3c). The weight of the films increased as the relative humidity in the chamber increased. Within two minutes of the humidity jump operation, the film reached an equilibrium state. This indicates that the PSSV rapidly absorbs moisture. The humidity dependence of the relative weight on the PSSV in the dry state (RH = 0%) is shown in Figure 3d. Here, the data in the high humidity range at RH > 60% were calculated using the saturated salt method for a bulk PSSV. The weight of PSSV increased continuously with increasing humidity, reaching a factor of approximately 2.2 at RH = 90%. The hygroscopic behavior of PSSV was similar to that of cationic linear polysiloxanes with ammonium salts, which has previously been reported [51].

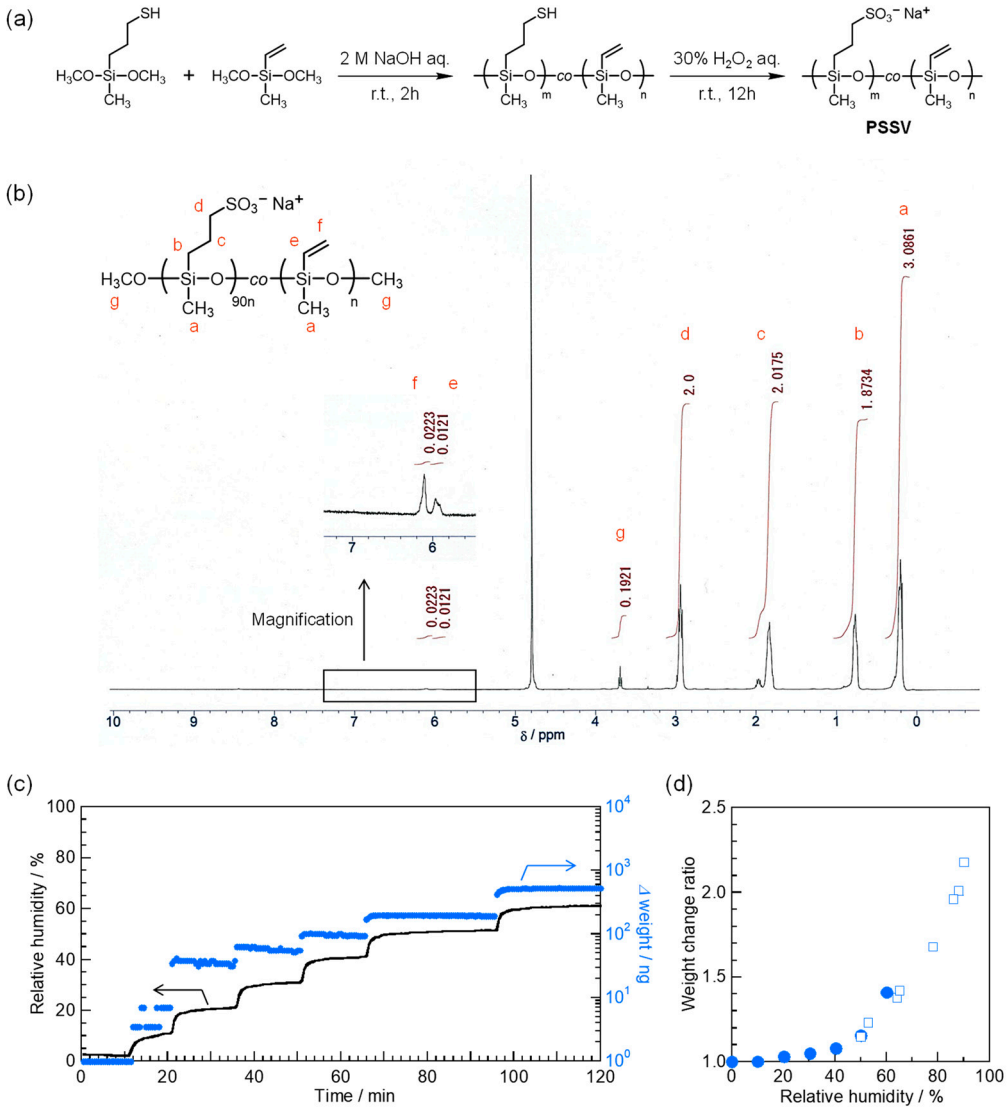


Figure 3. (**a**) Synthetic scheme to prepare anionic linear polysiloxane PSSV. (**b**) ^{1}H NMR spectrum of PSSV. (**c**) Time course profiles of the changes in relative humidity and weight change of PSSV film on QCM electrode. (**d**) Humidity-responsive weight change ratios of film-state PSSV (circle) and bulk-state PSSV (square).

3.3. Photoalignment of the BY Columnar Phase in PSSV Matrix Using LPVis Light

Figure 4a shows the polarized UV-vis absorption spectra of thin films composed of BY and PSSV when irradiated with LPVis light. The maximum absorption wavelength of the spectrum was blue-shifted by 5 nm from 410 nm by LPVis irradiation, and dichroism was also observed. It is likely that the presence of PSSV prevented BY from forming aggregates before LPVis irradiation, because no blue-shift phenomenon was observed when the pure BY film was irradiated with LPVis light. The S of the films irradiated with polarized visible light above 18 J cm^{-2} was 0.65–0.70 (Figure 4b), indicating that the BY columnar phase was highly photoaligned even in the PSSV matrix. GI-SAXS measurements also yielded data suggesting photoalignment of the BY columnar phase (Figure 4c,d). The periodic structure size after LPVis irradiation was also identical to that of the pure BY film, suggesting that the PSSV does not encompass each column, but bundles the domains of the BY columnar structure as shown in Figure 4e.

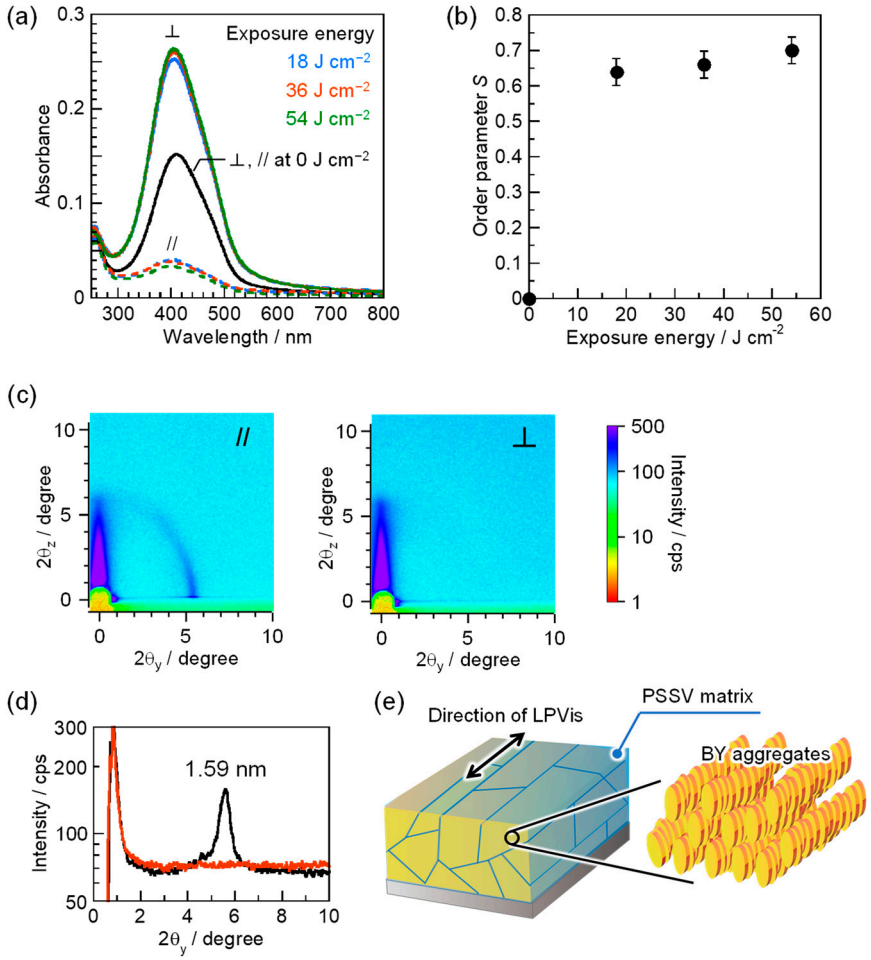


Figure 4. (**a**) Polarized UV-vis absorption spectra change of BY-PSSV films associated with exposure to LPVis light. (**b**) Order parameter change associated with dose of visible light. (**c**) GI-SAXS images of BY-PSSV films irradiated with LPVis light of 36 J cm^{-2} dose. X-ray beams were aligned to two directions parallel and perpendicular to the irradiated light. (**d**) In-plane intensity profiles of c. (**e**) Photoaligned BY columnar phase in PSSV matrix. PSSV is present in the blue region that bundles the BY domain.

3.4. UV Curing of the BY Columnar Phase in the PSSV Matrix

When the photoaligned BY columnar phase within the PSSV matrix was exposed to a RH level of 90% (show in route 1, Figure 5a), a red shift in the ππ* absorption band occurred (Figure 5b). As in the case of the pure BY film, it was considered that the BY columnar phase

was hydrated by the absorbed water, leading to the collapse in the photoalignment. The increase in time until S decreases compared to that in the pure BY film is considered to be because the PSSV matrix encapsulates the domains of the BY columnar phase and stabilizes the BY columnar phase. However, the decrease in S was more profound than that of the pure BY film. This may be due to the high hygroscopicity of PSSV, which enables a large amount of water to be incorporated into the film. Once the BY columnar phase begins to collapse, the orientation order is suddenly reduced after two hours. The GI-SAXS profiles of the film exposed to humidification also showed a peak (d = 1.91 nm) when the X-ray was incident perpendicular to the LPVis, suggesting a randomization of the photoaligned BY columnar phase. The peak position differs from that before humidification (Figure 4d) because the BY aggregates' transition takes place from the nematic columnar phase to the rectangular columnar phase due to humidification [39].

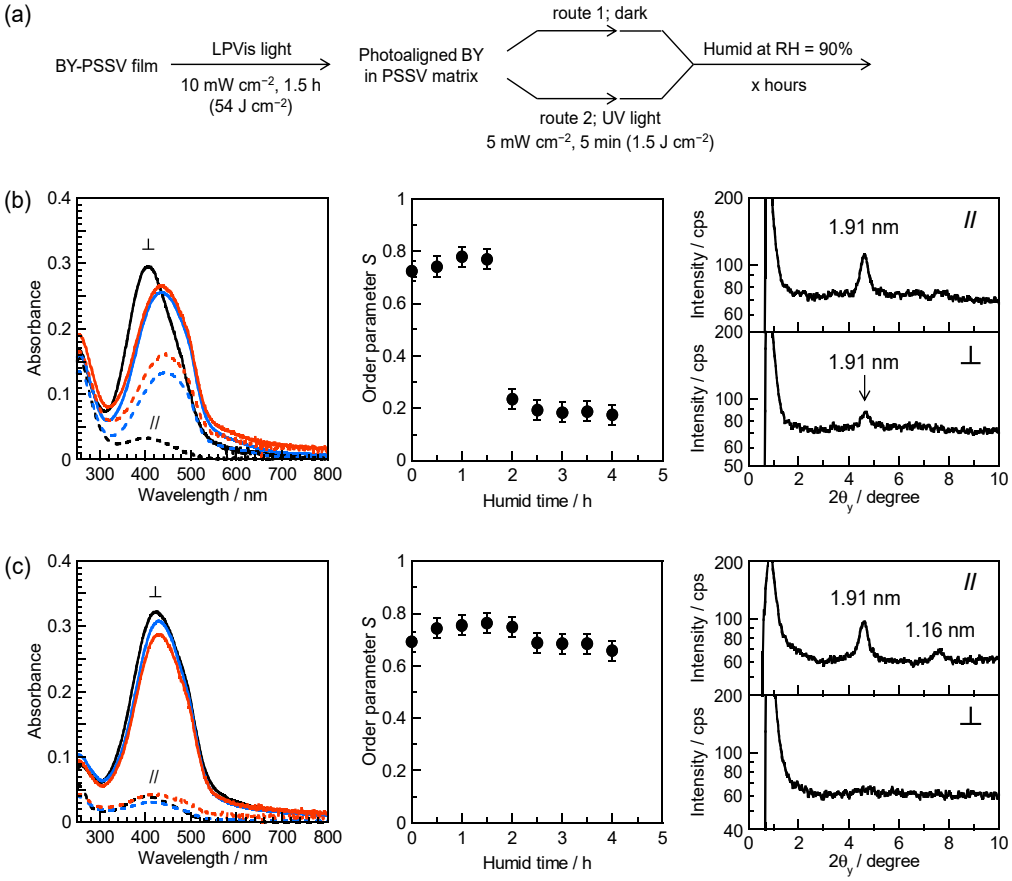


Figure 5. (**a**) Schematic procedure for BY-PSSV film. (**b**) Polarized UV-vis absorption spectra change (**left**), order parameter change (**center**), and in-plane profiles obtained by GI-SAXS measurements (**right**) with humidification at RH = 90% for BY-PSSV film passing through route 1. In the left figure of (**b**), black, blue, and brown lines indicate spectra after humidification of 0, 2, and 4 h, respectively. The right side profiles in (**b**) were obtained by GI-SAXS measurements after humidification of 2 h. (**c**) Data of BY-PSSV film passing through route 2, corresponding to (**b**).

Conversely, S was retained under the same humidity conditions when the UV-irradiated BY-PSSV film was exposed to a humid environment (route 2 in Figure 5a). Additionally, GI-SAXS measurements indicated that the photoalignment of the BY columnar phase was retained (Figure 5c). Thus, it was found that the photoaligned BY columnar phase could be firmly fixed by the crosslinking of PSSV. Figure 6a shows a visual photograph of the BY-PSSV film prepared on a quartz substrate after irradiation with LPVis and non-polarized UV lights, followed by further humidification at RH = 90% for 4 h. Figure 6b displays a photograph of the same film in Figure 6a, taken through a polarizer set above the film. The

color contrast of the film was significantly different when the direction of the transmitted light was perpendicular or parallel to direction of the LPVis light. In Figure 6c, the surface morphology of the film is shown. Some dotted protrusions were observed when compared to one of the pure BY film (see Figure 1a); however, overall, the surface of the BY-PSSV film was flat. These results indicate that it was possible to form the films on centimeter-scale substrates and to prepare large-area dichroic films even after humidification. Combined with pattern exposure through a photomask, various absorption anisotropic films can be developed. The film defects observed in Figure 6b were caused by repeatedly grabbing the film using tweezers during each humidification procedure and spectroscopic measurements.

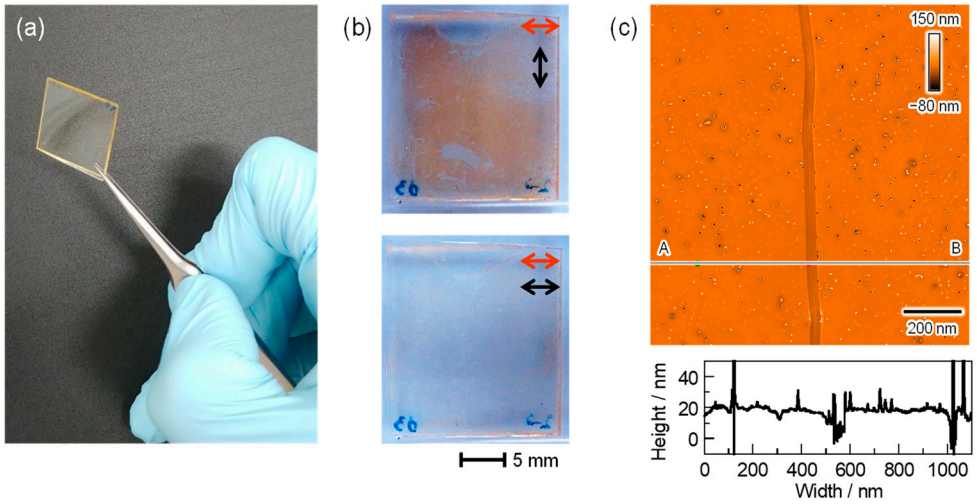


Figure 6. (**a**) Snapshot of BY-PSSV film on quartz. (**b**) Observation of BY-PSSV film through polarizer. The film was irradiated with an LPVis light of 36 J cm^{-2} dose and a UV light of 1.5 J cm^{-2} dose, then exposed to a humid atmosphere of RH = 90% for 4 h. Brown and black arrows indicate the directions of exposed LPVis light and polarizer, respectively. (**c**) Surface topographical morphology of the BY-PSSV film by white light interference microscopy. The cross-section of the average height profile along the A-B line in the top view image is shown below.

4. Conclusions

In this study, photoalignment and photo-fixation of the BY columnar phase were achieved using anionic linear polysiloxane PSSV as a matrix. Using light of two different wavelengths, the photoalignment and photo-fixation were independently achieved. PSSV bundles the domain of the BY columnar phase; thus, after the UV curing, the film dichroism remained as high as that of pure BY films, even after long-term exposure to the high-humidity environment. As the BY columnar phase is often used as photoalignment sublayers for low-molecular-mass nematic liquid crystals, this method, which improves the moisture resistance, is expected to expand the applications of BY. The BY alignment layer is also expected to be used as the alignment sublayer for water-soluble compounds. This proposal is expected to expand the possibilities of anisotropic materials for the alignment of water-soluble polymers, and for inducing molecular orientation of molecular aggregates in water media.

Author Contributions: M.H. and T.S. conceived and designed the project. A.M. conducted most of the experiments. S.N. provided experimental technical assistance and discussions on the data. M.H. and T.S. wrote the manuscript. All authors have read and agreed to the published version of the manuscript.

Funding: This work was supported by JSPS KAKENHI Grant Numbers JP18K14283, JP20H05217, JP22H02142, and JP22H04536 for MH, and JP21H01983 and JP21K19000 for TS. MH is also thankful for financial support from the Toshiaki Ogasawara Memorial Foundation, the Asahi Glass Foundation, and the Toukai Foundation for Technology.

Data Availability Statement: Not applicable.

Acknowledgments: We would like to thank Tatsuo Hikage of Nagoya University for their assistance with GI-SAXS measurements.

Conflicts of Interest: The authors declare no conflict of interest.

References

1. Kato, T.; Mizoshita, N.; Kishimoto, K. Functional Liquid-Crystalline Assemblies: Self-Organized Soft Materials. *Angew. Chem. Int. Ed.* **2006**, *45*, 38–68. [CrossRef] [PubMed]
2. Bukusoglu, E.; Bedolla Pantoja, M.; Mushenheim, P.C.; Wang, X.; Abbott, N.L. Design of Responsive and Active (Soft) Materials Using Liquid Crystals. *Annu. Rev. Chem. Biomol. Eng.* **2016**, *7*, 163–196. [CrossRef] [PubMed]
3. Kloos, J.; Joosten, N.; Schenning, A.; Nijmeijer, K. Self-assembling liquid crystals as building blocks to design nanoporous membranes suitable for molecular separations. *J. Membr. Sci.* **2021**, *620*, 118849. [CrossRef]
4. Uchida, J.; Soberats, B.; Gupta, M.; Kato, T. Advanced Functional Liquid Crystals. *Adv. Mater.* **2022**, *34*, 2109063. [CrossRef]
5. Bisoyi, H.K.; Li, Q. Liquid Crystals: Versatile Self-Organized Smart Soft Materials. *Chem. Rev.* **2022**, *122*, 4887–4926. [CrossRef]
6. Tam-Chang, S.-W.; Huang, L. Chromonic liquid crystals: Properties and applications as functional materials. *Chem. Commun.* **2008**, *17*, 1957–1967. [CrossRef]
7. Lydon, J. Chromonic review. *J. Mater. Chem.* **2010**, *20*, 10071–10099. [CrossRef]
8. Collings, P.J.; Goldstein, J.N.; Hamilton, E.J.; Mercado, B.R.; Nieser, K.J.; Regan, M.H. The nature of the assembly process in chromonic liquid crystals. *Liq. Cryst. Rev.* **2015**, *3*, 1–27. [CrossRef]
9. Dierking, I.; Martins Figueiredo Neto, A. Novel Trends in Lyotropic Liquid Crystals. *Crystals* **2020**, *10*, 604. [CrossRef]
10. Bosire, R.; Ndaya, D.; Kasi, R.M. Recent progress in functional materials from lyotropic chromonic liquid crystals. *Polym. Int.* **2021**, *70*, 938–943. [CrossRef]
11. Ichikawa, T.; Kuwana, M.; Suda, K. Chromonic Ionic Liquid Crystals Forming Nematic and Hexagonal Columnar Phases. *Crystals* **2022**, *12*, 1548. [CrossRef]
12. Schneider, T.; Lavrentovich, O.D. Self-Assembled Monolayers and Multilayered Stacks of Lyotropic Chromonic Liquid Crystalline Dyes with In-Plane Orientational Order. *Langmuir* **2000**, *16*, 5227–5230. [CrossRef]
13. Iverson, I.K.; Casey, S.M.; Seo, W.; Tam-Chang, S.-W.; Pindzola, B.A. Controlling Molecular Orientation in Solid Films via Self-Organization in the Liquid-Crystalline Phase. *Langmuir* **2002**, *18*, 3510–3516. [CrossRef]
14. Hara, M.; Nagano, S.; Mizoshita, N.; Seki, T. Chromonic/Silica Nanohybrids: Synthesis and Macroscopic Alignment. *Langmuir* **2007**, *23*, 12350–12355. [CrossRef] [PubMed]
15. Park, S.-K.; Kim, S.-E.; Kim, D.-Y.; Kang, S.-W.; Shin, S.; Kuo, S.-W.; Hwang, S.-H.; Lee, S.H.; Lee, M.-H.; Jeong, K.-U. Polymer-Stabilized Chromonic Liquid-Crystalline Polarizer. *Adv. Funct. Mater.* **2011**, *21*, 2129–2139. [CrossRef]
16. Ichimura, K. Photoalignment of Liquid-Crystal Systems. *Chem. Rev.* **2000**, *100*, 1847–1873. [CrossRef]
17. Seki, T.; Nagano, S.; Hara, M. Versatility of photoalignment techniques: From nematics to a wide range of functional materials. *Polymer* **2013**, *54*, 6053–6072. [CrossRef]
18. Priimagi, A.; Barrett, C.J.; Shishido, A. Recent twists in photoactuation and photoalignment control. *J. Mater. Chem. C* **2014**, *2*, 7155–7162. [CrossRef]
19. Ichimura, K.; Fujiwara, T.; Momose, M.; Matsunaga, D. Surface-assisted photoalignment control of lyotropic liquid crystals. Part 1. Characterization and photoalignment of aqueous solutions of a water-soluble dye as lyotropic liquid crystals. *J. Mater. Chem.* **2002**, *12*, 3380–3386. [CrossRef]
20. Fujiwara, T.; Ichimura, K. Surface-assisted photoalignment control of lyotropic liquid crystals. Part 2. Photopatterning of aqueous solutions of a water-soluble anti-asthmatic drug as lyotropic liquid crystals. *J. Mater. Chem.* **2002**, *12*, 3387–3391. [CrossRef]
21. Hara, M.; Nagano, S.; Kawatsuki, N.; Seki, T. Photoalignment and patterning of a chromonic-silica nanohybrid on photocrosslinkable polymer thin films. *J. Mater. Chem.* **2008**, *18*, 3259–3263. [CrossRef]
22. Van der Asdonk, P.; Hendrikse, H.C.; Fernandez-Castano Romera, M.; Voerman, D.; Ramakers, B.E.I.; Löwik, D.W.P.M.; Sijbesma, R.P.; Kouwer, P.H.J. Patterning of Soft Matter across Multiple Length Scales. *Adv. Funct. Mater.* **2016**, *26*, 2609–2616. [CrossRef]
23. Guo, Y.; Jiang, M.; Peng, C.; Sun, K.; Yaroshchuk, O.; Lavrentovich, O.D.; Wei, Q.-H. Designs of Plasmonic Metamasks for Photopatterning Molecular Orientations in Liquid Crystals. *Crystals* **2017**, *7*, 8. [CrossRef]
24. Wani, O.M.; Zeng, H.; Wasylczyk, P.; Priimagi, A. Programming Photoresponse in Liquid Crystal Polymer Actuators with Laser Projector. *Adv. Opt. Mater.* **2018**, *6*, 1700949. [CrossRef]
25. Wang, J.; McGinty, C.; Reich, R.; Finnemeyer, V.; Clark, H.; Berry, S.; Bos, P. Process for a Reactive Monomer Alignment Layer for Liquid Crystals Formed on an Azodye Sublayer. *Materials* **2018**, *11*, 1195. [CrossRef]
26. Berteloot, B.; Nys, I.; Poy, G.; Beeckman, J.; Neyts, K. Ring-shaped liquid crystal structures through patterned planar photoalignment. *Soft Matter* **2020**, *16*, 4999–5008. [CrossRef] [PubMed]
27. Yin, K.; Xiong, J.; He, Z.; Wu, S.-T. Patterning Liquid-Crystal Alignment for Ultrathin Flat Optics. *ACS Omega* **2020**, *5*, 31485–31489. [CrossRef]
28. Kim, K.; Kim, S.-U.; Choi, S.; Heo, K.; Ahn, S.-K.; Na, J.-H. High-Definition Optophysical Image Construction Using Mosaics of Pixelated Wrinkles. *Adv. Sci.* **2020**, *7*, 2002134. [CrossRef]

29. Nys, I.; Berteloot, B.; Poy, G. Surface Stabilized Topological Solitons in Nematic Liquid Crystals. *Crystals* **2020**, *10*, 840. [CrossRef]
30. Xiong, J.; Wu, S.-T. Planar liquid crystal polarization optics for augmented reality and virtual reality: From fundamentals to applications. *eLight* **2021**, *1*, 3. [CrossRef]
31. Kim, H.; Abdelrahman, M.K.; Choi, J.; Kim, H.; Maeng, J.; Wang, S.; Javed, M.; Rivera-Tarazona, L.K.; Lee, H.; Ko, S.H.; et al. From Chaos to Control: Programmable Crack Patterning with Molecular Order in Polymer Substrates. *Adv. Mater.* **2021**, *33*, 2008434. [CrossRef] [PubMed]
32. Padmini, H.N.; Rajabi, M.; Shiyanovskii, S.V.; Lavrentovich, O.D. Azimuthal Anchoring Strength in Photopatterned Alignment of a Nematic. *Crystals* **2021**, *11*, 675. [CrossRef]
33. Folwill, Y.; Zeitouny, Z.; Lall, J.; Zappe, H. A practical guide to versatile photoalignment of azobenzenes. *Liq. Cryst.* **2021**, *48*, 862–872. [CrossRef]
34. McGinty, C.P.; Kołacz, J.; Spillmann, C.M. Large rewritable liquid crystal pretilt angle by in situ photoalignment of brilliant yellow films. *Appl. Phys. Lett.* **2021**, *119*, 141111. [CrossRef]
35. Liu, S.; Nys, I.; Neyts, K. Two-Step Photoalignment with High Resolution for the Alignment of Blue Phase Liquid Crystal. *Adv. Opt. Mater.* **2022**, *10*, 2200711. [CrossRef]
36. Pinchin, N.P.; Lin, C.-H.; Kinane, C.A.; Yamada, N.; Pena-Francesch, A.; Shahsavan, H. Plasticized liquid crystal networks and chemical motors for the active control of power transmission in mechanical devices. *Soft Matter* **2022**, *18*, 8063–8070. [CrossRef] [PubMed]
37. Lall, J.; Zappe, H. In situ, spatially variable photoalignment of liquid crystals inside a glass cell using brilliant yellow. In Proceedings of the Photosensitive Materials and their Applications II, Strasbourg, France, 3 April–23 May 2022; Volume 12151.
38. Li, Y.; Luo, Z.; Wu, S.-T. High-Precision Beam Angle Expander Based on Polymeric Liquid Crystal Polarization Lenses for LiDAR Applications. *Crystals* **2022**, *12*, 349. [CrossRef]
39. Matsumori, M.; Takahashi, A.; Tomioka, Y.; Hikima, T.; Takata, M.; Kajitani, T.; Fukushima, T. Photoalignment of an Azobenzene-Based Chromonic Liquid Crystal Dispersed in Triacetyl Cellulose: Single-Layer Alignment Films with an Exceptionally High Order Parameter. *ACS Appl. Mater. Interfaces* **2015**, *7*, 11074–11078. [CrossRef] [PubMed]
40. Wang, J.; McGinty, C.; West, J.; Bryant, D.; Finnemeyer, V.; Reich, R.; Berry, S.; Clark, H.; Yaroshchuk, O.; Bos, P. Effect of humidity and surface on photoalignment of brilliant yellow. *Liq. Cryst.* **2016**, *44*, 863–872. [CrossRef]
41. Shi, Y.; Zhao, C.; Ho, J.Y.-L.; Vashchenko, V.V.; Srivastava, A.K.; Chigrinov, V.G.; Kwok, H.-S.; Song, F.; Luo, D. Exotic Property of Azobenzensulfonic Photoalignment Material Based on Relative Humidity. *Langmuir* **2017**, *33*, 3968–3974. [CrossRef]
42. Shi, Y.; Zhao, C.; Ho, J.Y.-L.; Song, F.; Chigrinov, V.G.; Luo, D.; Kwok, H.-S.; Sun, X.W. High Photoinduced Ordering and Controllable Photostability of Hydrophilic Azobenzene Material Based on Relative Humidity. *Langmuir* **2018**, *34*, 4465–4472. [CrossRef] [PubMed]
43. Wan, Y.; Zhao, D. On the Controllable Soft-Templating Approach to Mesoporous Silicates. *Chem. Rev.* **2007**, *107*, 2821–2860. [CrossRef] [PubMed]
44. Hara, M. Mesostructure and orientation control of lyotropic liquid crystals in a polysiloxane matrix. *Polym. J.* **2019**, *51*, 989–996. [CrossRef]
45. Huo, Q.; Margolese, D.I.; Ciesla, U.; Feng, P.; Gier, T.E.; Sieger, P.; Leon, R.; Petroff, P.M.; Schüth, F.; Stucky, G.D. Generalized synthesis of periodic surfactant/inorganic composite materials. *Nature* **1994**, *368*, 317–321. [CrossRef]
46. Hara, M.; Orito, T.; Nagano, S.; Seki, T. Humidity-responsive phase transition and on-demand UV-curing in a hygroscopic polysiloxane-surfactant nanohybrid film. *Chem. Commun.* **2018**, *54*, 1457–1460. [CrossRef]
47. Hara, M.; Wakitani, N.; Kodama, A.; Nagano, S.; Seki, T. Hierarchical Photocomposition of Heteronanostructures in a Surfactant-Polysiloxane Hybrid Film toward Next-Generation Nanolithography. *ACS Appl. Polym. Mater.* **2020**, *2*, 2284–2290. [CrossRef]
48. Kaneko, Y. Ionic silsesquioxanes: Preparation, structure control, characterization, and applixations. *Polymer* **2018**, *144*, 205–224. [CrossRef]
49. Kaneko, Y.; Toyodome, H.; Mizumo, T.; Shikinaka, K.; Iyi, N. Preparation of a Sulfo-Group-Containing Rod-Like Polysilsesquioxane with a Hexagonally Stacked Structure and Its Proton Conductivity. *Chem. Eur. J.* **2014**, *20*, 9394–9399. [CrossRef]
50. Hara, M.; Ueno, Y.; Nagano, S.; Seki, T. Water-Retentive/Lipophilic Amphiphilic Surface Properties Attained by Hygroscopic Polysiloxane Ultrathin Films. *J. Fiber Sci. Technol.* **2022**, *78*, 169–177. [CrossRef]
51. Hara, M.; Iijima, Y.; Nagano, S.; Seki, T. Simple linear ionic polysiloxane showing unexpected nanostructure and mechanical properties. *Sci. Rep.* **2021**, *11*, 17683. [CrossRef]

Disclaimer/Publisher's Note: The statements, opinions and data contained in all publications are solely those of the individual author(s) and contributor(s) and not of MDPI and/or the editor(s). MDPI and/or the editor(s) disclaim responsibility for any injury to people or property resulting from any ideas, methods, instructions or products referred to in the content.